

Available at www.sciencedirect.com

ScienceDirect

journal homepage: www.elsevier.com/locate/carbon

Plasma enhanced growth of single walled carbon nanotubes at low temperature: A reactive molecular dynamics simulation

M. Shariat ^{a,b}, S.I. Hosseini ^c, B. Shokri ^{a,d}, E.C. Neyts ^{e,*}^a Shahid Beheshti University, Laser and Plasma Research Institute, G.C., Evin, Tehran, Iran^b Valie Asr University, Department of Physics, Rafsanjan, Iran^c Shahrood University of Technology, Department of Physics, 36155 Shahrood, Iran^d Shahid Beheshti University, Department of Physics, G.C., Evin, Tehran, Iran^e University of Antwerp, Research Group PLASMANT, Department of Chemistry, 2610 Wilrijk, Antwerp, Belgium

ARTICLE INFO

Article history:

Received 13 June 2013

Accepted 17 August 2013

Available online 23 August 2013

ABSTRACT

Low-temperature growth of carbon nanotubes (CNTs) has been claimed to provide a route towards chiral-selective growth, enabling a host of applications. In this contribution, we employ reactive molecular dynamics simulations to demonstrate how plasma-based deposition allows such low-temperature growth. We first show how ion bombardment during the growth affects the carbon dissolution and precipitation process. We then continue to demonstrate how a narrow ion energy window allows CNT growth at 500 K. Finally, we also show how CNTs in contrast cannot be grown in thermal CVD at this low temperature, but only at high temperature, in agreement with experimental data.

© 2013 Elsevier Ltd. All rights reserved.

1. Introduction

Growth of carbon nanotubes (CNTs) in general and single walled CNTs (SWCNTs) in particular continues to attract widespread attention thanks to their specific electrical, mechanical, physical and chemical properties. These properties give rise to a host of envisaged applications in diverse areas including electronics, energy storage, composite materials and medical industry, to name just a few [1]. Interestingly, SWCNTs may be either conducting or semiconducting, depending on their chirality, allowing their use in electronic devices such as transistors, interconnects, sensors, etc. [1–3]. The ability to control the SWCNT chirality is thus of primary importance. Until now, however, chirality-controlled growth remains an elusive goal. Moreover, recent molecular dynamics simulations demonstrated that SWCNT chirality can be altered after the initial cap formation, by the introduc-

tion of defects [4]. On the other hand, a number of studies have also demonstrated partial chiral selectivity [5–9]. One route often envisaged to accomplish further chiral selectivity, is epitaxial growth [10–13]. This, however, requires the growth to proceed from a seed or nanoparticle with crystalline structure, prohibiting the high temperatures typically required for SWCNT growth. Alternatively, recent DFT simulations pointed out that also a strong metal/catalyst interaction may impose a structure on the catalyst nanoparticle which may also lead to epitaxial growth [14].

At present, the most popular technique to grow CNTs is chemical vapor deposition (CVD) [15,16]. The lowest temperature recorded to date for growing SWCNTs thermally is 350 °C (623 K), by Cantoro and et al. [17]. Note, however, that various factors besides the temperature also contribute to growth or non-growth, including the particle size and work of adhesion [14,18,19].

* Corresponding author.

E-mail address: erik.neyts@uantwerpen.be (E.C. Neyts).

0008-6223/\$ - see front matter © 2013 Elsevier Ltd. All rights reserved.

<http://dx.doi.org/10.1016/j.carbon.2013.08.025>

An interesting alternative is plasma enhanced CVD (PECVD), both for MWCNTs as well as SWCNTs [20–27]. The PECVD system is characterized by a number of parameters not available to thermal CVD, such as the plasma power, bias voltage, and the external electric and magnetic fields, as well as by other parameters including the chamber geometry, gas pressure and temperature. The availability of these additional parameters holds promise to obtain a better control over the growth and thus the properties of the tubes. Indeed, these additional parameters control the density and energy of the plasma species (electrons, ions, excited species and active radicals), all of which contribute to the SWCNT nucleation and growth.

One example of the use of PECVD-specific factors to our advantage is the use of electric fields to grow vertically aligned freestanding SWCNTs [27–29]. Another interesting advantage of PECVD is that it allows growing CNTs at reduced temperatures relative to thermal growth, which is a key parameter for growth on temperature sensitive substrates like polymers and plastics. Moreover, this also provides the ability of selective growth (synthesises carbon nanotubes with selective diameter distributions) [30]. The lowest temperatures which have been reported for MWCNT and SWCNT growth are 120 °C and 400 °C, respectively [31,32]. A more detailed account of the various effects and advantages of PECVD can be found in recent reviews [33,34].

The growth process of SWCNTs and the underlying dynamics has been studied on the atomic level using classical MD and MD/MC simulations [4,18,19,35–43], as well as using ab initio and semi ab initio techniques [44–48]. The majority of these works, however, correspond to thermal CVD.

Indeed, due to the complex chemical reactions occurring in plasma, the mechanistic details of the PECVD growth process are at present far from understood. Recently, Neyts et al. investigated the effects of electric field [49] and Ar ion bombardment [50] on the growth process of CNTs in the plasma at the atomic level by hybrid MD/force-biased MC (MD/fbMC) simulations [51,52]. Their results showed how applying an electric field assists SWCNTs to grow in the direction of the electric field. They also found that Ar ion bombardment in a limited but well-defined energy window of 10–25 eV leads to better nucleation and defect healing of the SWCNT cap. In

this work, we study for the first time the nucleation and growth of SWCNTs under low temperature plasma conditions. It should be mentioned that a full representation of the plasma-based growth setup would also include the presence of a carrier gas, neutral molecule growth precursor gas, gas phase atoms, metastable species, radicals, ions, electrons and photons, in addition to electric and possibly magnetic fields [53]. In order to disentangle the various effects and to keep the simulation complexity feasible, we here only investigate the effect of ions during the growth and specifically in relation to the required growth temperature. Other types of simulation, however, have taken into account the multitude of factors and processes in PECVD growth, albeit not at the atomic scale [54,55].

A simple schematic of a typical PECVD reactor is shown in Fig. 1a. In such a reactor the plasma is ignited and sustained by applying either a DC voltage or RF power. As mentioned above, the plasma environment contains various species such as electrons, ions, radicals and molecules. If the density of electrons and ions are equal, the plasma is quasi-neutral. This condition is valid in the bulk of plasma. The much higher mobility of electrons than ions results in a depletion of the electron density near the electrodes, leading to the formation of a positive charge region – called the plasma sheath – in front of the electrodes. This in turn induces a voltage drop parallel to the electrodes in front of the electrodes and thus a strong electric field in that region electric field (Fig. 1b). In Fig. 1b, the boundaries of the sheaths are indicated by the dashed lines. The ions are accelerated in the sheath region by this field, and as result the kinetic energy of the ions may reach up to several hundred eV (Fig. 1b).

It should also be mentioned that at low temperature the energy and flux of ions are two key parameters in sputtering of amorphous carbon which may cover the catalyst surface [26,56]. This amorphous carbon prevents incoming growth precursors to be absorbed to the catalyst surface and thus suppresses nanotube growth at low temperature. It should also be noted that if the ion energy and density is too high, the ions can even sputter the catalyst particle and fully developed SWCNTs on the substrate which is detrimental for the growth [26]. Under these conditions, MWCNTs show more resistance against ion irradiation and remain attached to

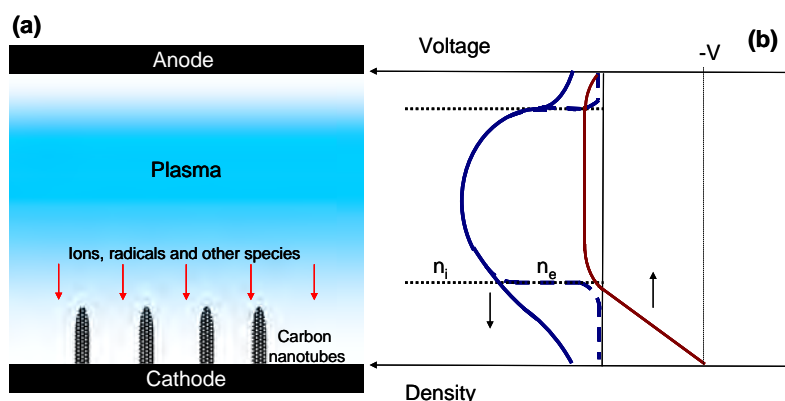


Fig. 1 – (a) Simplified schematic of a plasma-enhanced CVD reactor, (b) potential distribution in the plasma (red line) and density of ions (solid blue line) and electrons (dashed blue line). (A color version of this figure can be viewed online.)

the substrate [57]. Therefore, it is crucial to design the appropriate plasma environment for the growth of nanostructures, e.g. by using a remote downstream plasma enhanced CVD [31,58] or atmospheric pressure plasma setup [29]. Finally, the collisions of the energetic ions with the catalyst may cause local heating of the catalyst. While tuning the ion density and energy, it should be realized that the number density of hydrocarbon radicals is two or three orders of magnitude higher than that of the hydrocarbon ions. Neutral molecules (and radicals) are therefore usually considered as the main source of carbon atoms for the formation of nanotubes [24,59]. Thus, there is a competition between the carbon generation and deposition by radical species and carbon sputtering by ions.

2. Methodology

Our simulation model is very similar to the model originally developed by Ding et al. [60] for investigating the nucleation and growth of SWCNTs in thermal CVD. The Fe–Fe and Fe–C interactions are thus described by a sum of Born–Mayer repulsive and attractive terms, and the Johnson potential, respectively [61]. Our model differs from their model only in the use of the improved second-generation reactive empirical bond order potential developed by Brenner et al. [62] and modified by Ito and Nakamura [63] for describing precipitated carbon atoms. In this model, there are two classes of carbon atoms: (1) the carbon atoms dissolved in the metal cluster, and (2) the precipitated carbon atoms which cover the surface

of the cluster and eventually grow into a nanotube. In our simulations, the catalyst particle is a metallic Fe cluster containing 48 atoms. It is first annealed for 100 ps at the desired temperature, after which carbon atoms were allowed to impinge on the cluster every 40 ps. The trajectories were integrated by the Verlet Velocity algorithm using a time step of 0.5 fs. In the CVD simulations, SWCNT growth was studied at 500 K (which is more than 100 K below the lowest growth temperature recorded to date) and 1100 K (which is a typical growth temperature).

In the PECVD simulations, thermal carbon atoms or energetic carbon ions are added to the Fe cluster every 30 ps. The ions are assumed to be neutralized by Auger emission before their actual impact with the surface. Here, the flux of carbon atoms is approximately equal to that of thermal CVD, because the pressure is assumed to be equal to thermal CVD. Carbon atoms that are added to the cluster with thermal velocity correspond to carbon atoms originating from surface-decomposition of hydrocarbon gas, while the carbon atoms added to the cluster with higher velocities correspond to carbon ions (accelerated in the plasma sheath).

It is also assumed that the number of all the neutral hydrocarbon species, including the radicals, excited species, and neutral molecules, are four times higher than that of the hydrocarbon ions. Thus, each fifth carbon species added to the cluster is a carbon ion, while the other four are thermal carbon atoms. The simulated PECVD growth is carried out at low temperature (500 K), employing the Berendsen thermostat [64] with a relaxation time of 0.01 ps to control the

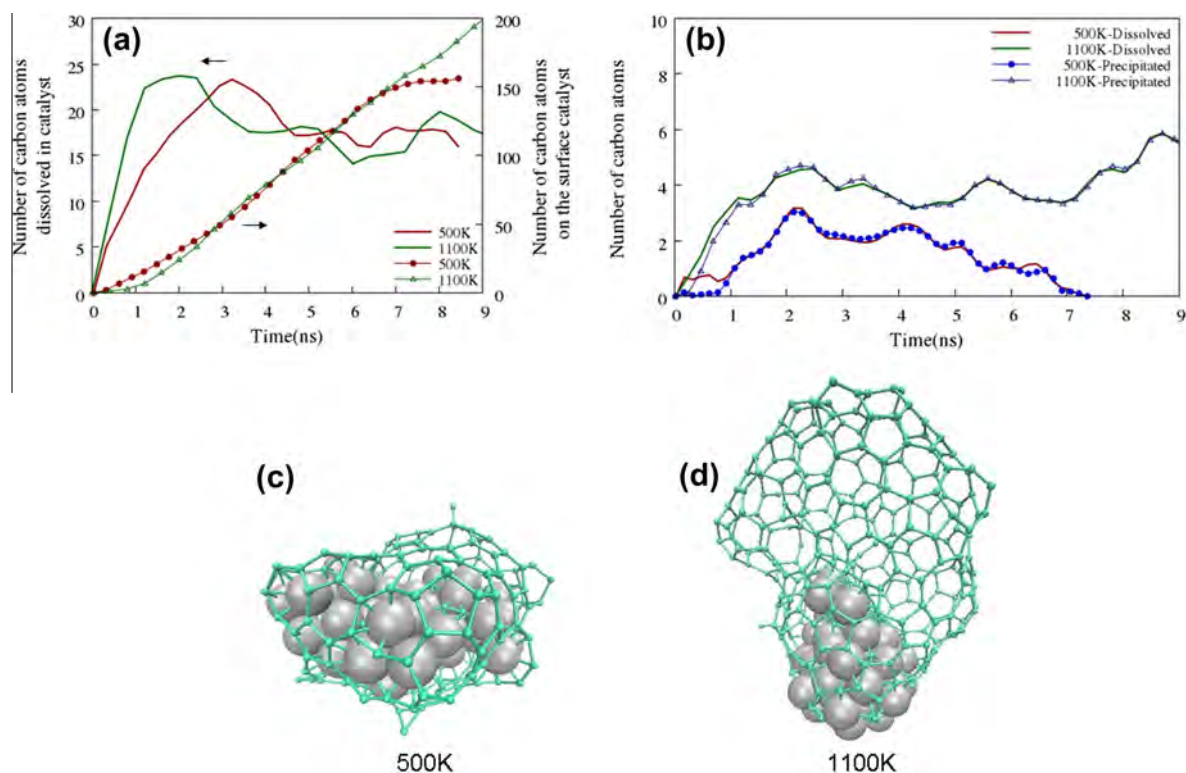


Fig. 2 – A snapshot of the simulated CVD growth of SWCNTs at 500 K and 1100 K. The small green atoms and the large grey atoms are carbon and iron atoms, respectively. (A color version of this figure can be viewed online.)

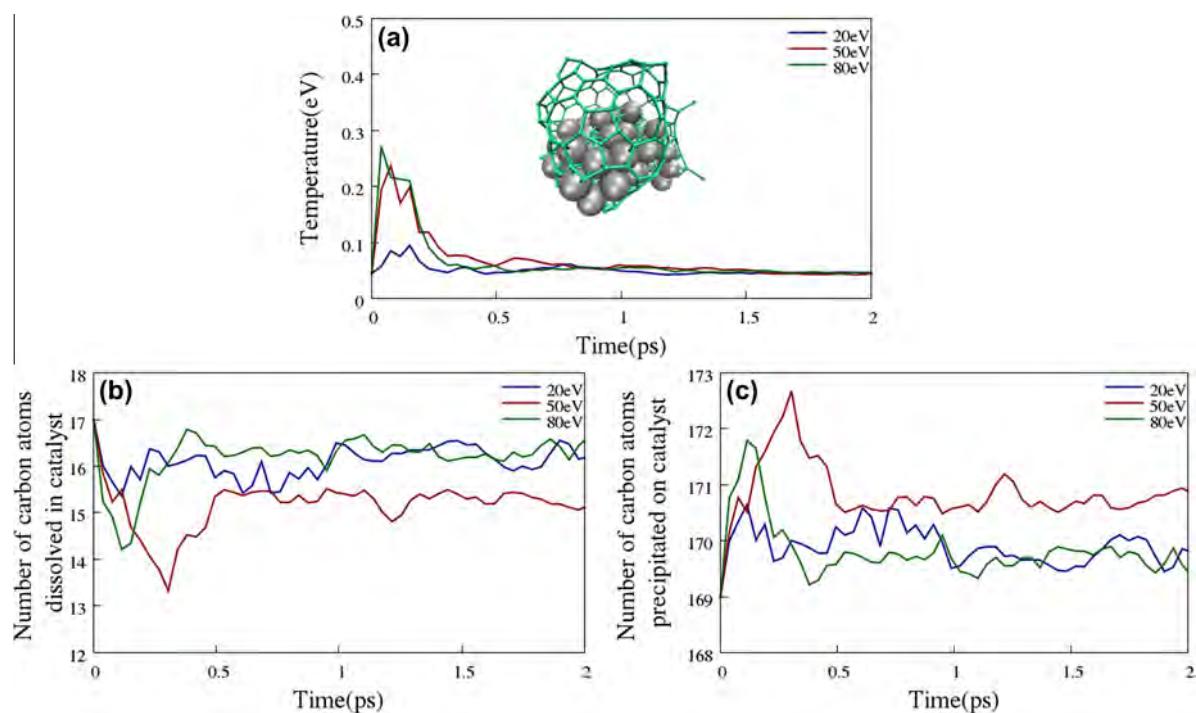


Fig. 3 – Effect of C-ion impinging on the Fe₄₆C₁₈₆ cluster: evolution of (a) the metal cluster temperature, (b) the number of dissolved carbon atoms, and (c) the number of deposited carbon atoms on the surface of the catalyst particle. (A color version of this figure can be viewed online.)

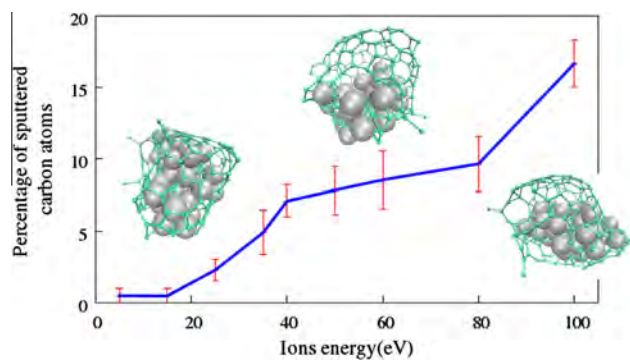


Fig. 4 – Percentage of sputtered carbon atoms by ions energy. (A color version of this figure can be viewed online.)

temperature. It should be noted that during the initial impact period of the ion with the catalyst, the thermostat is turned off for 150 fs, corresponding to an isolated system. After this period, the atoms which do not participate in the collision are coupled to the heat bath. After 1 ps and after removing the sputtered species from the simulation cell, the thermostat is turned on again for all atoms. This procedure aims to mimic a strongly cooled catalyst, to ensure growth at the targeted low temperature, thus avoiding excessive heating due to the ion bombardment. While the Berendsen thermostat does not rigorously reproduce the canonical ensemble (although it does correspond to an NVT simulation), the resulting processes in similar simulations were found to be

very similar to those obtained when using the canonical Bussi thermostat [65].

The time step for the initial stages of the impact is 0.05 fs, increasing up to 0.5 fs with decreasing maximum velocity. Ion impact energies of 5, 15, 35, 40, 50, 60, 80 and 100 eV are applied, and each run is carried out five times to gather statistics.

Note that MD simulations are inherently restricted to relatively short time scales, such that the obtained growth rates in any MD simulation are far too high. The essential processes and mechanisms, however, are captured by the simulation. Also note that due to these short time scales, thermodynamic equilibrium can obviously not be reached. However, thermodynamic effects such as the Gibbs–Thomson effect or the size-dependent solubility of carbon in the nanocluster is naturally taken into account by virtue of the force field, provided at least that the force field is sufficiently accurate.

3. Results and discussion

3.1. Simulated CVD growth

In the CVD method, the temperature is the key parameter in the growth of nanotubes. The effects of temperature have been investigated in detail in earlier simulation works by other researchers [18,66]. Our results are in good agreement with those studies. Fig. 2a shows the dissolution of carbon atoms in the metal cluster. It can be seen that the carbon concentration in the cluster first increases steeply. Subsequently, a supersaturation stage is reached, after which the dissolved

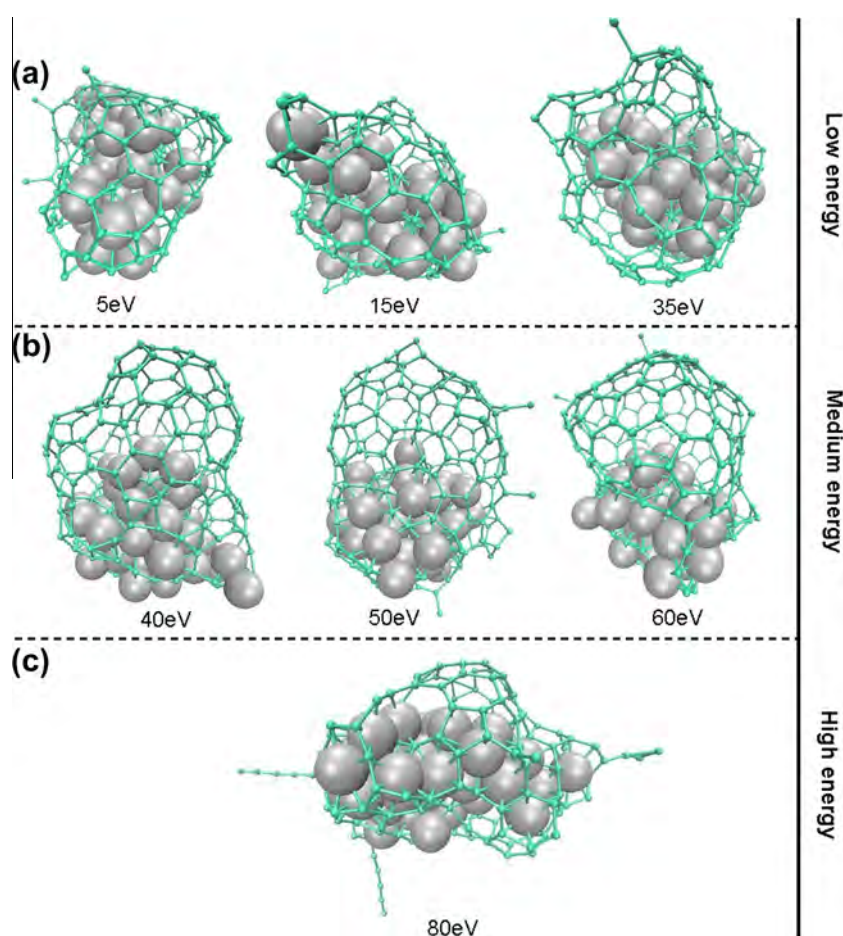


Fig. 5 – The growth of a SWCNT for different ion energies. (A color version of this figure can be viewed online.)

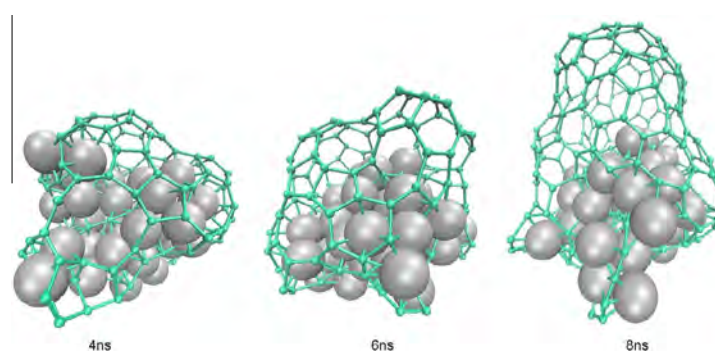


Fig. 6 – Snapshots of SWCNT growth under C-ion irradiation with ion energy of 40 eV at 500 K. (A color version of this figure can be viewed online.)

carbon atoms start to precipitate until the structure reaches an equilibrium state. In this process, a (defective) graphitic network is seen to emerge, in agreement with previous calculations. This graphene layer subsequently forms a cap and finally detaches from the catalyst surface. In this stage, the added carbon atoms at the surface of the metal catalyst attach to the cap structure, from which the CNT can continuously grow (Fig. 2d). As can be seen in Fig. 2a, the behavior of the dissolved carbon atoms is similar at both low (500 K) and high (1100 K) temperatures, but there is a marked difference in the evolution of the precipitated carbon atoms. In-

deed, whereas the number of precipitated carbon atoms continuously increases at 1100 K, this number quickly is saturated after complete saturation of the cluster at 500 K. Thus, at low temperature, the carbon network simply covers the surface of the nanoparticle, thereby deactivating the catalyst. Therefore, nanotubes cannot grow by the CVD method at low temperature (Fig. 2c).

Fig. 2b shows the number of carbon atoms that are dissolving in cluster and precipitating on the surface of the nanoparticle as a function of time. At both temperatures, the initial dissolution rate is higher than the precipitation rate, thus

leading to an increase in the number of dissolved carbon atoms. After supersaturation stage, carbon atom dissolution rate becomes equal to the precipitation rate. At low temperature, however, both rates decrease to 0, due to the encapsulation of the nanoparticle.

3.2. Simulated PECVD growth

In the PECVD method, the energy and flux of the ions are of special importance in the growth process. In the present work we explore the possibility of low temperature growth by PECVD and the effects of ion energy on the growth process.

As a first step, we investigate the collision of a single carbon ion with energies of 20, 50 and 80 eV with a $\text{Fe}_{46}\text{C}_{186}$ cluster thermalized at 500 K. The temperature of the metal cluster as a function of time is shown in Fig. 3. It can be seen in the figure that the temperature of the cluster shows a spike in the first 0.5 ps, due to the ion impact and the rapid subsequent heat dissipation. During the initial temperature spike, i.e., during the impact of the ion, the number of dissolved carbon atoms steeply decreases. The ion impinging thus leads to a very fast precipitation of carbon during the first 0.25 ps after the moment of impact. After this initial period, however, the spike dies off and the carbon atoms dissolve in the cluster again. At low ion energy (20 eV), the change in temperature and the number of dissolved and precipitated carbon atoms is very limited (Fig. 3). Therefore, the fluctuations in temperature and number of dissolved and precipitated atoms are not due to turning off the thermostat.

After relaxation of the collision, the number of dissolved carbon atoms in the catalyst has decreased slightly overall (Fig. 3b), i.e., the collision effectively leads to the precipitation of one or a few carbon atoms on the surface, contributing to the formation of a graphitic structure. Especially at moderate energy (50 eV), the number of precipitated carbon atoms increases significantly (Fig. 3c).

Figs. 4 and 5 show the percentage of sputtered carbon atoms versus impinging ion energy, and the overall growth result at different ion energies at 500 K, respectively. As ex-

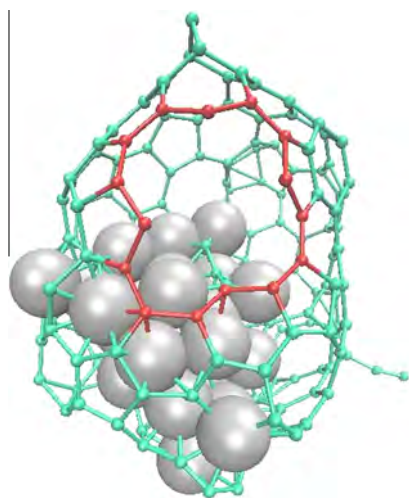


Fig. 7 – High ion energies create multiple defects in the nucleated SWCNT cap. (A color version of this figure can be viewed online.)

pected, the percentage of sputtered carbon atoms increases with increasing ion energy. The overall growth is found to exhibit an optimum at moderate energy, as discussed below.

3.2.1. Low ion energy (<35 eV)

When the energy of the impinging ions is low, their effect is small and the growth process is very similar to CVD growth (Fig. 2c). An extended graphitic structure forms on the surface of the nanocatalyst, which prevents the addition of new carbon atoms to the catalyst. In this condition, the energy of the ions is not sufficient to break bonds in the amorphous network or sputter the network (Fig. 4). Thus, at this low temperature, the process does not result in the formation of a cap that can detach from the surface and lead to growth of a nanotube (Fig. 5a).

3.2.2. Moderate ion energies (35–60 eV)

When the impinging ions have an energy in the order of 35–60 eV, we find that the SWCNTs can be nucleated and grow at 500 K (see Fig. 5b). The carbon network covers a part of the nanoparticle surface but the ions prevent this network to cover all of surface, by displacement and sputtering amorphous carbon atoms. In this stage, the added carbon atoms at the surface of the metal catalyst form a cap, from which the CNT can continuously grow. In this energy window, the ion energy is not too high to sputter the carbon atoms already incorporated in the cap/nanotube (Fig. 4), but it is sufficiently high to break amorphous carbon bonds, thereby preventing poisoning of the metal nanoparticle which is essential for continued growth of nanotubes (Fig. 6).

3.2.3. High ion energy (≥ 80 eV)

At this condition, the percentage of sputtered carbon atoms is very high (Fig. 4). Even some Fe atoms are sputtered in the initial stage of the process. Also carbon atoms already incorporated in the nanotube structure are seen to be sputtered, as shown in Fig. 7. At this condition, a strong increase in the local temperature is observed as well (see Fig. 3a). The high energy impacts, however, lead to the formation of many defects in the cap structure. In this range of ion energies, SWCNT caps are found to be able to nucleate, but they are quickly sputtered, preventing their further growth into an actual SWCNT (Fig. 5c).

4. Conclusions

In this work we investigated SWCNT growth under both CVD and PECVD conditions. In the CVD method, nanotubes could be grown at a temperature of 1100 K, whereas only a graphitic layer grew on the surface of catalyst particle at a low temperature of 500 K. In PECVD, however, growth at this lower temperature is found to be feasible, provided that ions with an appropriate energy (35–60 eV) are present that bombard the surface of the catalyst. For energies lower than this range, the growth mechanism behaves very similar to the CVD method and a graphitic encapsulating structure was formed on the surface. For ion energies above this range, large amounts of carbon

atoms, including atoms already incorporated in the CNT, were sputtered from the structure. The energy of the impinging ions is thus a key parameter in growing SWCNTs in a PECVD-setup, enabling growth at low temperatures.

REFERENCES

- [1] Harris PJF. Carbon nanotube science: synthesis, properties and applications. Cambridge University Press Cambridge; 2009.
- [2] Tans SJ, Verschueren ARM, Dekker C. Room-temperature transistor based on a single carbon nanotube. *Nature* 1998;393(6680):49–52.
- [3] Odom TW, Huang J-L, Kim P, Lieber CM. Atomic structure and electronic properties of single-walled carbon nanotubes. *Nature* 1998;391(6662):62–4.
- [4] Neyts EC, Van Duin ACT, Bogaerts A. Changing chirality during single-walled carbon nanotube growth: a reactive molecular dynamics/monte carlo study. *J Am Chem Soc* 2011;133(43):17225–31.
- [5] Bachilo SM, Balzano L, Herrera JE, Pompeo F, Resasco DE, Weisman RB. Narrow (N, M)-distribution of single-walled carbon nanotubes grown using a solid supported catalyst. *J Am Chem Soc* 2003;125(37):11186–7.
- [6] Chiang W-H, Sankaran RM. Linking catalyst composition to chirality distributions of As-grown single-walled carbon nanotubes by tuning Nixfe1–X nanoparticles. *Nat Mater* 2009;8(11):882–6.
- [7] Fouquet M, Bayer B, Esconjauregui S, Blume R, Warner J, Hofmann S, et al. Highly chiral-selective growth of single-walled carbon nanotubes with a simple monometallic Co catalyst. *Phys Rev B* 2012;85(23):235411.
- [8] He M, Chernov AI, Fedotov PV, Obratsova ED, Sainio J, Rikkinen E, et al. Predominant (6, 5) single-walled carbon nanotube growth on a copper-promoted iron catalyst. *J Am Chem Soc* 2010;132(40):13994–6.
- [9] He M, Jiang H, Liu B, Fedotov PV, Chernov AI, Obratsova ED, et al. Chiral-selective growth of single-walled carbon nanotubes on lattice-mismatched epitaxial cobalt nanoparticles. *Sci Rep* 2013;3.
- [10] Koziol KK, Ducati C, Windle AH. Carbon nanotubes with catalyst controlled chiral angle. *Chem Mater* 2010;22(17):4904–11.
- [11] Reich S, Li L, Robertson J. Control the chirality of carbon nanotubes by epitaxial growth. *Chem Phys Lett* 2006;421(4):469–72.
- [12] Shibuta Y. A numerical approach to the metal-catalyzed growth process of carbon nanotubes. *Diam Relat Mater* 2011;20(3):334–8.
- [13] Zhu H, Suenaga K, Wei J, Wang K, Wu D. A strategy to control the chirality of single-walled carbon nanotubes. *J Cryst Growth* 2008;310(24):5473–6.
- [14] Gómez-Gualdrón DA, Zhao J, Balbuena PB. Nanocatalyst structure as a template to define chirality of nascent single-walled carbon nanotubes. *J Chem Phys* 2011;134:14705.
- [15] Ducati C, Alexandrou I, Chhowalla M, Amaratunga GAJ, Robertson J. Temperature selective growth of carbon nanotubes by chemical vapor deposition. *J Appl Phys* 2002;92(6):3299–303.
- [16] Maruyama S, Einarsson E, Murakami Y, Edamura T. Growth process of vertically aligned single-walled carbon nanotubes. *Chem Phys Lett* 2005;403(4):320–3.
- [17] Cantoro M, Hofmann S, Pisana S, Scardaci V, Parvez A, Ducati C, et al. Catalytic chemical vapor deposition of single-wall carbon nanotubes at low temperatures. *Nano Lett* 2006;6(6):1107–12.
- [18] Burgos JC, Reyna H, Yakobson BI, Balbuena PB. Interplay of catalyst size and metal-carbon interactions on the growth of single-walled carbon nanotubes. *J Phys Chem C* 2010;114(15):6952–8.
- [19] Ribas MA, Ding F, Balbuena PB, Yakobson BI. Nanotube nucleation versus carbon-catalyst adhesion-probed by molecular dynamics simulations. *J Chem Phys* 2009;131:224501.
- [20] Kato T, Hatakeyama R. Direct growth of short single-walled carbon nanotubes with narrow-chirality distribution by time-programmed plasma chemical vapor deposition. *ACS Nano* 2010;4(12):7395–400.
- [21] San Hua L, Zhiqiang L, Zexiang S, Jianyi L. Plasma-assisted synthesis of carbon nanotubes. *Nanoscale Res Lett* 2010;5:1377–86.
- [22] Gohier A, Minea TM, Djouadi MA, Jimenez J, Granier A. Growth kinetics of low temperature single-wall and few walled carbon nanotubes grown by plasma enhanced chemical vapor deposition. *Physica E* 2007;37(1):34–9.
- [23] Song IK, Cho YS, Choi GS, Park JB, Kim DJ. The growth mode change in carbon nanotube synthesis in plasma-enhanced chemical vapor deposition. *Diam Relat Mater* 2004;13(4):1210–3.
- [24] Kato T, Hatakeyama R, Tohji K. Diffusion plasma chemical vapour deposition yielding freestanding individual single-walled carbon nanotubes on a silicon-based flat substrate. *Nanotechnology* 2006;17(9):2223.
- [25] Kato T, Jeong GH, Hirata T, Hatakeyama R, Tohji K, Motomiya K. Single-walled carbon nanotubes produced by plasma-enhanced chemical vapor deposition. *Chem Phys Lett* 2003;381(3):422–6.
- [26] Luo Z, Lim S, You Y, Miao J, Gong H, Zhang J, et al. Effect of ion bombardment on the synthesis of vertically aligned single-walled carbon nanotubes by plasma-enhanced chemical vapor deposition. *Nanotechnology* 2008;19(25):255607.
- [27] Maschmann MR, Amama PB, Goyal A, Iqbal Z, Fisher TS. Freestanding vertically oriented single-walled carbon nanotubes synthesized using microwave plasma-enhanced CVD. *Carbon* 2006;44(13):2758–63.
- [28] Chhowalla M, Teo KBK, Ducati C, Rupesinghe NL, Amaratunga GAJ, Ferrari AC, et al. Growth process conditions of vertically aligned carbon nanotubes using plasma enhanced chemical vapor deposition. *J Appl Phys* 2001;90(10):5308–17.
- [29] Nozaki T, Ohnishi K, Okazaki K, Kortshagen U. Fabrication of vertically aligned single-walled carbon nanotubes in atmospheric pressure non-thermal plasma CVD. *Carbon* 2007;45(2):364–74.
- [30] Ionescu MI, Zhang Y, Li R, Sun X. Selective growth, characterization, and field emission performance of single-walled and few-walled carbon nanotubes by plasma enhanced chemical vapor deposition. *Appl Surf Sci* 2011;258(4):1366–72.
- [31] Bae EJ, Min YS, Kang D, Ko JH, Park W. Low-temperature growth of single-walled carbon nanotubes by plasma enhanced chemical vapor deposition. *Chem Mater* 2005;17(20):5141–5.
- [32] Hofmann S, Ducati C, Robertson J, Kleinsorge B. Low-temperature growth of carbon nanotubes by plasma-enhanced chemical vapor deposition. *Appl Phys Lett* 2003;83(1):135–7.
- [33] Meyyappan M. A review of plasma enhanced chemical vapour deposition of carbon nanotubes. *J Phys D: Appl Phys* 2009;42(21):213001.

- [34] Neyts EC. PECVD growth of carbon nanotubes: from experiment to simulation. *J Vacuum Sci Technol B: Microelectr Nanometer Struct* 2012;30(3):30803–17.
- [35] Balbuena PB, Zhao J, Huang S, Wang Y, Sakulchaicharoen N, Resasco DE. Role of the catalyst in the growth of single-wall carbon nanotubes. *J Nanosci Nanotechnol* 2006;6(5):1247–58.
- [36] Burgos JC, Jones E, Balbuena PB. Effect of the metal-substrate interaction strength on the growth of single-walled carbon nanotubes. *J Phys Chem C* 2011;115(15):7668–75.
- [37] Ding F, Rosén A, Bolton K. Molecular dynamics study of the catalyst particle size dependence on carbon nanotube growth. *J Chem Phys* 2004;121:2775.
- [38] Ding F, Rosén A, Bolton K. Dependence of SWNT growth mechanism on temperature and catalyst particle size: bulk versus surface diffusion. *Carbon* 2005;43(10):2215–34.
- [39] Gómez-Gualdrón DA, Mckenzie GD, Alvarado JFJ, Balbuena PB. Dynamic evolution of supported metal nanocatalyst/carbon structure during single-walled carbon nanotube growth. *ACS Nano* 2011;6(1):720–35.
- [40] Shibuta Y, Maruyama S. Molecular dynamics simulation of formation process of single-walled carbon nanotubes by CCVD method. *Chem Phys Lett* 2003;382(3):381–6.
- [41] Shibuta Y, Elliott JA. A molecular dynamics study of the carbon–catalyst interaction energy for multi-scale modelling of single wall carbon nanotube growth. *Chem Phys Lett* 2006;427(4):365–70.
- [42] Neyts EC, Shibuta Y, Van Duin ACT, Bogaerts A. Catalyzed growth of carbon nanotube with definable chirality by hybrid molecular dynamics-force biased Monte Carlo simulations. *ACS Nano* 2010;4(11):6665.
- [43] Neyts EC, Shibuta Y, Bogaerts A. Bond switching regimes in nickel and nickel–carbon nanoclusters. *Chem Phys Lett* 2010;488(4):202–5.
- [44] Amara H, Bichara C, Ducastelle F. Interaction of carbon clusters with Ni (100): application to the nucleation of carbon nanotubes. *Surf Sci* 2008;602(1):77–83.
- [45] Börjesson A, Bolton K. First principles studies of the effect of ostwald ripening on carbon nanotube chirality distributions. *ACS Nano* 2011;5(2):771–9.
- [46] Ding F, Harutyunyan AR, Yakobson BI. Dislocation theory of chirality-controlled Nanotube growth. *Proc Natl Acad Sci* 2009;106(8):2506–9.
- [47] Ohta Y, Okamoto Y, Irlé S, Morokuma K. Rapid growth of a single-walled carbon nanotube on an iron cluster: density-functional tight-binding molecular dynamics simulations. *ACS Nano* 2008;2(7):1437–44.
- [48] Page AJ, Ohta Y, Irlé S, Morokuma K. Mechanisms of single-walled carbon nanotube nucleation, growth, and healing determined using QM/MD methods. *Acc Chem Res* 2010;43(10):1375–85.
- [49] Neyts EC, Van Duin ACT, Bogaerts A. Insights in the plasma-assisted growth of carbon nanotubes through atomic scale simulations: effect of electric field. *J Am Chem Soc* 2012;134(2):1256–60.
- [50] Neyts EC, Ostrikov K, Han ZJ, Kumar S, Van Duin ACT, Bogaerts A. Defect healing and enhanced nucleation of carbon nanotubes by low-energy ion bombardment. *Phys Rev Lett* 2013;110(6):65501.
- [51] Mees MJ, Pourtois G, Neyts EC, Thijsse BJ, Stesmans A. Uniform-acceptance force-bias Monte Carlo method with time scale to study solid-state diffusion. *Phys Rev B* 2012;85(13):134301.
- [52] Neyts EC, Thijsse BJ, Mees MJ, Bal KM, Pourtois G. Establishing uniform acceptance in force biased Monte Carlo simulations. *J Chem Theor Comput* 2012;8(6):1865–9.
- [53] Ostrikov K, Neyts E, Meyyappan M. Plasma nanoscience: from nano-solids in plasmas to nano-plasmas in solids. *Adv Phys* 2013;62(2):113–224.
- [54] Ostrikov K, Mehdipour H. Thin single-walled carbon nanotubes with narrow chirality distribution: constructive interplay of plasma and Gibbs–Thomson effects. *ACS Nano* 2011;5(10):8372–82.
- [55] Ostrikov K, Mehdipour H. Nanoscale plasma chemistry enables fast, size-selective nanotube nucleation. *J Am Chem Soc* 2012;134(9):4303–12.
- [56] Denysenko I, Ostrikov K, Yu MY, Azarenkov NA. Effects of ions and atomic hydrogen in plasma-assisted growth of single-walled carbon nanotubes. *J Appl Phys* 2007;102(7):074308–74310.
- [57] Gohier A, Minea TM, Djouadi AM, Granier A, Dubosc M. Limits of the PECVD process for single wall carbon nanotubes growth. *Chem Phys Lett* 2006;421(1):242–5.
- [58] Ohashi T, Kato R, Ochiai T, Tokune T, Kawarada H. High quality single-walled carbon nanotube synthesis using remote plasma CVD. *Diam Relat Mater* 2012.
- [59] Hash D, Bose D, Govindan TR, Meyyappan M. Simulation of the Dc plasma in carbon nanotube growth. *J Appl Phys* 2003;93(10):6284–90.
- [60] Ding F, Bolton K, Rosen A. Nucleation and growth of single-walled carbon nanotubes: a molecular dynamics study. *J Phys Chem B* 2004;108(45):17369–77.
- [61] Ding F, Bolton K, Rosén A. Iron-carbide cluster thermal dynamics for catalyzed carbon nanotube growth. *J Vacuum Sci Technol A: Vacuum, Surf, Films* 2004;22(4):1471–6.
- [62] Brenner DW, Shenderova OA, Harrison JA, Stuart SJ, Ni B, Sinnott SB. A second-generation reactive empirical bond order (REBO) potential energy expression for hydrocarbons. *J Phys: Condens Matter* 2002;14(4):783.
- [63] Ito A, Nakamura H. Molecular dynamics simulation of bombardment of hydrogen atoms on graphite surface. *Commun Comput Phys* 2008;4:592–610.
- [64] Berendsen HJC, Postma Jplm, Van Gunsteren WF, Dinola ARHJ, Haak JR. Molecular dynamics with coupling to an external bath. *J Chem Phys* 1984;81:3684.
- [65] Somers W, Bogaerts A, Van Duin ACT, Huygh S, Bal KM, Neyts EC. Temperature influence on the reactivity of plasma species on a nickel catalyst surface: an atomic scale study. *Catal Today* 2013;211:131–6.
- [66] Ding F, Rosen A, Campbell EEB, Falk LKL, Bolton K. Graphitic encapsulation of catalyst particles in carbon nanotube production. *J Phys Chem B* 2006;110(15):7666–70.